AD-A240 927

OFFICE OF NAVAL RESEARCH

Contract N00014-82K-0612

Task No. NR 627-838

TECHNICAL REPORT NO. 64

# Electrochemical Investigations of Electronically Conductive Polymers. VII. Charge-Transport in Lightly-Doped Polypyrrole

by

Zhihau Cai and Charles R. Martin

Department of Chemistry
Colorado State University
Ft. Collins, CO 80523

Prepared for publication

in

Synthetic Metals

September 13, 1991

Reproduction in whole or part is permitted for any purpose of the United States Government

*This document has been approved for public release and sale; its distribution is unlimited

*This statement whould also appear in Item 10 of Document Control Data - DD Form 1473. Copies of form Available from cognizant contract administrator

91-11438

91 6 24 092

SECURITY CLASSIFICATION OF THIS PAGE

# REPORT DOCUMENTATION PAGE

Form Approved OMB No. 0704-0188

| | |
|---|---|
| 1a. REPORT SECURITY CLASSIFICATION<br>UNCLASSIFIED | 1b. RESTRICTIVE MARKINGS |
| 2a. SECURITY CLASSIFICATION AUTHORITY | 3. DISTRIBUTION/AVAILABILITY OF REPORT<br>APPROVED FOR PUBLIC DISTRIBUTION, DISTRIBUTION UNLIMITED. |
| 2b. DECLASSIFICATION/DOWNGRADING SCHEDULE | |
| 4. PERFORMING ORGANIZATION REPORT NUMBER(S)<br>ONR TECHNICAL REPORT #64 | 5. MONITORING ORGANIZATION REPORT NUMBER(S) |
| 6a. NAME OF PERFORMING ORGANIZATION<br>Dr. Charles R. Martin<br>Department of Chemistry<br>6b. OFFICE SYMBOL (If applicable) | 7a. NAME OF MONITORING ORGANIZATION<br>Office of Naval Research |
| 6c. ADDRESS (City, State, and ZIP Code)<br>Colorado State University<br>Ft. Collins, CO 80523 | 7b. ADDRESS (City, State, and ZIP Code)<br>800 North Quincy Street<br>Arlington, VA 22217 |
| 8a. NAME OF FUNDING/SPONSORING ORGANIZATION<br>Office of Naval Research<br>8b. OFFICE SYMBOL (If applicable) | 9. PROCUREMENT INSTRUMENT IDENTIFICATION NUMBER<br>Contract # N00014-82K-0612 |
| 8c. ADDRESS (City, State, and ZIP Code)<br>800 North Quincy Street<br>Arlington, VA 22217 | 10. SOURCE OF FUNDING NUMBERS<br>PROGRAM ELEMENT NO. / PROJECT NO. / TASK NO / WORK UNIT ACCESSION NO |

11. TITLE (Include Security Classification)
Electrochemical Investigations of Electronically Conductive Polymers. VII. Charge-Transport in Lightly-Doped Polypyrrole

12. PERSONAL AUTHOR(S)
Zhihau Cai and Charles R. Martin

| 13a. TYPE OF REPORT | 13b. TIME COVERED | 14. DATE OF REPORT (Year, Month, Day) | 15. PAGE COUNT |
|---|---|---|---|
| Technical | FROM _____ TO _____ | 1991, 9, 5 | |

16. SUPPLEMENTARY NOTATION

| 17. COSATI CODES | | | 18. SUBJECT TERMS (Continue on reverse if necessary and identify by block number) |
|---|---|---|---|
| FIELD | GROUP | SUB-GROUP | Electronically conductive polymers, polypyrrole, synthetic metals |
| | | | |
| | | | |

19. ABSTRACT (Continue on reverse if necessary and identify by block number)

We and others have shown that the mechanism and rate of charge transport in polypyrrole films (on electrode surfaces) depend on whether the polymer is in its electronically conductive or electronically insulating state. This paper focuseson the mechanism and rate of charge transport in the electronically insulating state; i.e. we describe results of electrochemical investigations of polypyrrole films which were equilibrated at initial potentials negative of -0.30 V vs. SCE. With regard to mechanism of charge transport, we show that this lightly doped material behaves like a redox polymer. In particular, we show that like other redox polymers, redox reactions for lightly doped polypyrrole begin at the polymer/electrode interface and propagate to the polymer/solution interface. With regard to rate of charge transport, we show that apparent diffusion coefficients for polypyrrole synthesized from acetonitrile solutions containing 2% added water are significantly lower than charge transpor rates in films synthesized in rigorously-dried acetonitrile. Finally, we report exchange current densities associated with the oxidation of lightly doped polypyrrole. These exchange current densities are on the order of 4 mA $cm^{-2}$, indicating relatively facile electron transf kinetics.

| 20. DISTRIBUTION/AVAILABILITY OF ABSTRACT | 21. ABSTRACT SECURITY CLASSIFICATION |
|---|---|
| ☒ UNCLASSIFIED/UNLIMITED ☐ SAME AS RPT ☐ DTIC USERS | UNCLASSIFIED |
| 22a. NAME OF RESPONSIBLE INDIVIDUAL<br>Dr. Robert Nowak | 22b. TELEPHONE (Include Area Code)<br>(202) 696-4410 |
| | 22c. OFFICE SYMBOL |

DD Form 1473, JUN 86 *Previous editions are obsolete.* SECURITY CLASSIFICATION OF THIS PAGE

# ELECTROCHEMICAL INVESTIGATIONS OF ELECTRONICALLY CONDUCTIVE POLYMERS. VII. CHARGE-TRANSPORT IN LIGHTLY-DOPED POLYPYRROLE

Zhihua Cai and Charles R. Martin*

Department of Chemistry
Colorado State University
Fort Collins, CO 80523

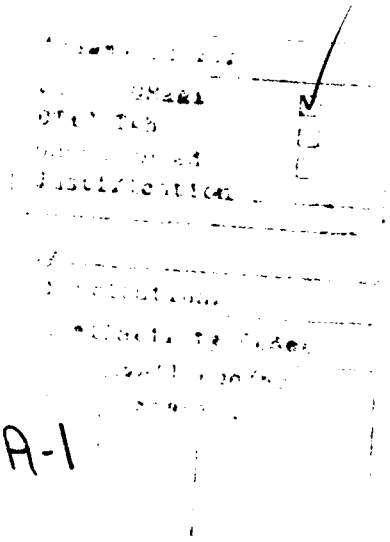


*Corresponding author

099

## ABSTRACT

We and others have shown that the mechanism and rate of charge transport in polypyrrole films (on electrode surfaces) depend on whether the polymer is in its electronically conductive or electronically insulating state. This paper focuses on the mechanism and rate of charge transport in the electronically insulating state; i.e. we describe results of electrochemical investigations of polypyrrole films which were equilibrated at initial potentials negative of -0.30 V vs. SCE. With regard to mechanism of charge transport, we show that this lightly doped material behaves like a redox polymer. In particular, we show that like other redox polymers, redox reactions for lightly doped polypyrrole begin at the polymer/electrode interface and propagate to the polymer/solution interface. With regard to rate of charge transport, we show that apparent diffusion coefficients for polypyrrole synthesized from acetonitrile solutions containing 2 % added water are significantly lower than charge transport rates in films synthesized in rigorously-dried acetonitrile. Finally, we report exchange current densities associated with the oxidation of lightly doped polypyrrole. These exchange current densities are on the order of 4 mA $cm^{-2}$, indicating relatively facile electron transfer kinetics.

# INTRODUCTION

Electronically conductive polymers can be reversibly switched between electronically insulating (or semiconducting) and electronically conductive states (1,2). For polypyrrole (and other polyheterocyclics) this switching reaction can be written as

$$-[M]_y- \; + \; n\,X_s^- \; \text{-----} > \; -[(M^+\,X^-)_n\text{-}(M_{(y-n)})]- \; + \; n\,e^- \quad (1)$$

where M and $M^+$ are neutral (i.e. reduced) and oxidized monomer units in the polymer phase and $X^-$ is an anion initially present in a contacting solution phase. The neutral polymer on the left side of Equation 1 is the electronically insulating state and the polycation on the right side is the electronically conductive state.

The redox process shown in Equation 1 is usually accomplished electrochemically by coating the polypyrrole film onto an inert electrode surface (1,2). Equation 1 entails injection of charge into the polymer phase and transport of this charge throughout the bulk polymer. Ion transport accompanies this charge transport process. We have been interested in the mechanisms and rates of these charge and ion transport processes (3-6). We, and others, have shown that the mechanism of charge transport depends on whether the polymer is in its electronically insulating or electronically conductive states (3-8). When the polymer is electronically conductive, charge transport occurs uniformly throughout the bulk of the polymer phase via a capacitive-like mechanism (4,8). Thus, from an electrochemical viewpoint, the polymer resembles a porous metal (9). In contrast, when the polymer is in its insulating state, charge is injected at one of the film's surfaces and charge is then transported into the bulk via a diffusional process (5,6). Thus, in this state, the polymer resembles a redox polymer (10,11).

For the insulating material, there is still some disagreement as to whether the polymer redox reaction (Equation 1) begins at the polymer/electrode interface or the polymer/solution interface (12,13). For example, Lee et al. present ellipsometric data which suggest that the redox reaction begins at the polymer/solution interface and works inward to the polymer/electrode interface (12); in contrast, Tezuka and Aoki's data suggest that, in analogy to a redox polymer, charge injection begins at the polymer/electrode interface and works outward to the polymer/solution interface (13). Furthermore, the potential region in which the charge injection process changes from the interfacial mechanism (nonconductive material) to the porous metal mechanism (conductive material) is not well defined.

We have used a series of chronopotentiometric experiments, in conjunction with in situ measurements of electronic conductivity, to address these issues. The data obtained suggest that the polymer oxidation process begins at the polymer/electrode interface. The chronopotentiometric method also provides the apparent diffusion coefficient, which is a quantitative measure of the rate of the diffusive charge-transport process (5,6), and the exchange current for the interfacial electron transfer process. The results of these experiments are described here.

## EXPERIMENTAL

Materials and Instrumentation. Pyrrole (Aldrich 99 %) was distilled twice under $N_2$, immediately prior to use. Tetraethylammonium tetrafluoroborate (Aldrich 99 %) was recrystallized twice from methanol (Baker Analyzed) and then dried in vacuo at room temperature for 12 hours and then at 100° C for 24 hrs. Acetonitrile (Burdick Jackson, UV grade) and all other reagents were used as received. Pt disk working electrodes (diameter =

1 mm) were constructed and pretreated as described previously (4). A 6 mm diameter Pt disk coated with a 0.5 $\mu$m-thick polypyrrole film was used as the counter electrode; the rationale for this unusual counter electrode was discussed in our previous paper (4). A conventional saturated calomel electrode (SCE) was used as the reference. The electrochemical instrumentation and cell were described previously (4). All potentials quoted in this paper are vs. SCE.

Film Deposition. Polypyrrole films were synthesized from a $CH_3CN$ solution which was 0.5 M in pyrrole, 0.2 M in $Et_4NBF_4$, and 2 % in water. Water was added to the polymerization solution because Diaz and others suggest that such low concentrations of water improve the mechanical properties of the polymer and the adhesion of the film to the electrode surface (14-16). We will show here, however, that polypyrrole films obtained from these water-containing solutions support lower rates of charge transport than films synthesized in acetonitrile that does not contain deliberately-added water (5,6). Polymerization was accomplished galvanostatically at a current density of 1.0 mA $cm^{-2}$. Reproducible steady-state potentials of $0.79\pm0.01$ V were observed during deposition. The thickness of the polypyrrole film was controlled by varying the charge passed during polymerization (4).

After synthesis, the film-coated electrode was removed from the polymerization solution and rinsed thoroughly with Ar-degassed $CH_3CN$. The electrode was then immersed into a $CH_3CN$ solution containing the desired concentration of supporting electrolyte ($Et_4NBF_4$). Prior to performing other measurements, cyclic voltammetry was routinely used to assess the quality of the freshly-synthesized films (4).

In Situ Measurement of Electronic Conductivity. We have developed a simple in situ method for measuring the electronic conductivity of polypyrrole as a function of applied potential. This method uses the bipotentiostatic cell shown in Figure 1. The film-coated electrode was immersed into supporting electrolyte solution and equilibrated at the desired initial electrode potential. Care was taken to protect the film from air because lightly doped polypyrrole is extremely susceptible to irreversible oxidation by $O_2$ (17). After equilibration, the film-coated electrode was brought into contact with the Pt disk electrode. The second half of the bipotentiostat was used to apply a 5 mV bias between the film-coated electrode and the lower Pt disk electrode and measure the resulting current.

In order to minimize contact resistance, a pressure of ca. 200 psi was applied between the film-coated and the lower Pt disk electrodes. This pressure was arrived at via a study of effect of applied pressure on the current between the film-coated and lower Pt disk electrodes. Current increased with applied pressure but leveled at pressure of 200 psi or higher. The electronic conductivity of the film ($\sigma_e$) was calculated from the measured current, i, via

$$\sigma_e = i\, d/(AV) \qquad (2)$$

where d is the film thickness, A is the film area and V is the bias between the electrodes.

In Situ Measurement of Ionic Conductivity. We have recently developed a current pulse method for measuring the ionic conductivities of highly-conductive polymer films (18). This method entails recording the potential-time transient following application of a short duration current pulse at the film-coated electrode. The film-coated electrode was immersed into the supporting electrolyte solution and equilibrated at the desired initial potential A current

pulse (1 mA $cm^{-2}$ x 100 $\mu$s) was then applied to the working electrode and the resulting potential-time transient was recorder with a digital oscilloscope.

We have shown that at short times, the potential-time transient is given by (18)

$$E(t) - E(0) = (R_t)\, i_p + i_p t/C_d \qquad (3)$$

where E(t) is the potential at time t after application of the pulse, E(0) is the initial applied potential, $R_t$ is the sum of the resistance of the polymer film ($R_f$) and the resistance of the contacting solution phase ($R_s$), $i_p$ is the magnitude of the current pulse, and $C_d$ is the capacitance of the double layer at the film/electrode interface. Equation 3 assumes that, in this very short time window, the potential vs. time transient is associated with charging of the double layer at the film/working electrode interface (18). In agreement with Equation 3, the experimental transients show an extended region of linear behavior (Figure 2).

Equation 3 indicates that the film resistance ($R_f$) can be obtained by extrapolating the linear portion of the potential-time transient (Figure 2) to t=0. The solution resistance must, however, be know. The solution resistance was measured by conducting analogous current pulse experiments at a bare Pt disk working electrode. The ionic conductivity of the polypyrrole film was calculated from the measured $R_f$ and the (known) thickness and area of the film (18).

Measurement of the Apparent Diffusion Coefficient and Exchange Current Density for Lightly-Doped Polypyrrole. Apparent diffusion coefficients (5,6) were also measured via a current pulse experiment. However, the time scale for this experiment was approximately three orders of magnitude longer than the time scale of the current pulse experiment described in the previous section. The polypyrrole film-coated working electrode was

immersed in supporting electrolyte and equilibrated at the desired initial potential. The electrode was then switched to open circuit and an anodic current pulse (0.5 sec, amplitude ranging from 150 to 600 $\mu$A $cm^{-2}$) was applied. The resulting potential-time transient was recorded.

Typical potential-time transients are shown in Figure 3. Note, again, that the time scale of this experiment is significantly longer than the time scale of the experiment described in the previous section (compare time axes in Figures 2 and 3). On the time scale shown in Figure 3, the double layer has already been charged, and the injected charge is now used to create excess (relative to the initial equilibrium potential) oxidized monomer sites. We will show below that these oxidized sites are created at the Pt/film interface. The potential-time transient in Figure 3 is associated with the transport of these oxidized sites into the bulk of the film (i.e with equilibration of the concentration of oxidized sites).

In this lightly-doped regime this equilibration process occurs via electron hopping from reduced to oxidized sites in the polypyrrole film (5,6). In analogy to redox polymers, electron hopping in lightly-doped polypyrrole can be modeled as a diffusional process. Thus, the concentration of oxidized sites at the substrate electrode surface ($C_{M+}(x=0)$) at any time, t, after application of the current pulse can be described by (19)

$$C_{M+}(x=0) = C^{*}_{M+} + \frac{2\, i_s\, t^{0.5}}{F\, A\, \pi^{0.5}\, D_e^{0.5}} \qquad (4)$$

where $C^{*}_{M+}$ is the initial concentration of oxidized sites, $i_s$ is the magnitude of the current pulse, and $D_e$ is the apparent diffusion coefficient.

If, in response to the applied current pulse, the magnitude of the potential change is less tnan ca. 60 mV, the linearized potential-concentration relation obtains (20)

$$E(t) - E(0) = i_s R_t + \frac{RT}{F}\left(\frac{C_{M+}(x=0)}{C^{\bullet}_{M+}} - \frac{C_M(x=0)}{C_M^{\bullet}} + \frac{i_s}{i_o}\right) \quad (5)$$

where $C_M(x=0)$ is the concentration of reduced (i.e. neutral) monomer sites at the electrode/film interface, $C_M^{\bullet}$ is the bulk concentration of reduced monomer sites in the film, and $i_o$ is the exchange current (20). Because we are beginning with lightly doped polypyrrole and the extent of oxidation by the current pulse is kept low, $C_M(x=0)/C_M^{\bullet}$ is approximately unity. Thus, combining Equations 4 and 5 gives

$$E(t) - E(0) = i_s\left(R_t + \frac{RT}{i_oF}\right) + \frac{RT}{F}\left(\frac{2i_st^{0.5}}{FA\pi^{0.5}D_e^{0.5}C_{M+}^{\bullet}}\right) \quad (6)$$

Equation 6 predicts that potential after application of the current pulse will vary linearly with the square root of time. Figure 4 shows that this is, indeed, the case. The exchange current can be obtained from the intercept of the linear potential vs. $t^{0.5}$ plot, provided $R_t$ is known. As indicated above, $R_t$ is determined independently. The apparent diffusion coefficient, $D_e$, can be obtained from the slope of the linear potential vs. $t^{0.5}$ plot, provided the concentration of oxidized sites at the initial potential, E(0), is known. The relationship between applied potential and $C^{\bullet}_{M+}$ was obtained using a coulometric titration method (6).

A plot of potential vs. $\log C^{\bullet}_{M+}$ obtained via this coulometric titration method (6) is shown in Figure 5. As has been observed by us (6) and others (21) this plot is linear (at low doping levels) and supernernstian. The $C^{\bullet}_{M+}$ data shown in Figure 5 were used, in

conjunction with Equation 6, to obtain apparent diffusion coefficients for charge-transport in the lightly doped polypyrrole films. In addition, the data in Figure 5 can be used to calculate the doping level at any value of E(0) via

$$\text{doping level (\%)} = 100\ C^{\bullet}_{M+} / C^{\bullet} \qquad (7)$$

where $C^{\bullet}$ is the total concentration of monomer units in the polymer film.

## RESULTS AND DISCUSSION

### What is the Mechanism by Which Undoped or Lightly-Doped Polypyrrole is Oxidized?

Figure 5 shows a cyclic voltammogram for the reduced (undoped) form of polypyrrole. The film, in this case, was 0.52 $\mu$m thick; voltammograms for films up to 3 $\mu$m in thickness were qualitatively similar. Figure 6 shows that when the potential of the substrate electrode is scanned positively, the undoped material is oxidized and ultimately converted to the conductive form. This paper focuses on results of electrochemical experiments conducted after equilibration of the polymer film at potentials negative of -0.30 V; i.e. we focus on the undoped and lightly doped material. The objective of this section of this paper is to determine the mechanism by which this material is oxidized.

As indicated in the Introduction, this oxidation process could, in principle, occur via three different mechanisms (12). In analogy to a redox polymer, oxidation could begin at the Pt/polymer interface with oxidized equivalents being transported into the bulk of the polymer via electron hopping (5,6). Tezuka and Aoki's data support this model (13). Alternatively, oxidation could proceed from the polymer/solution interface. While this at first glance might seem unlikely, it is important to point out that undoped polypyrrole is a semiconductor. For example, the conductivity of a film equilibrated at -0.35 V is ca. $10^{-5}\ \Omega^{-1}\ cm^{-1}$ (22). This

conductivity means that a film which is 0.5 $\mu$m thick with an area of 1 $cm^2$ would have a resistance of only 5 $\Omega$. Thus, an oxidation process initiated at the polymer/solution interface followed by transport of electrons through the film via an electronic conduction mechanism does not seem inconceivable. Furthermore, ellipsometric data obtained by Lee et al. (12) support this "outside-in" mechanism.

The final possible mechanism for polymer oxidation assumes that oxidation occurs uniformly throughout the bulk of the material; i.e. this mechanism assumes that the polymer is like a porous metal. We have shown that when polypyrrole is in its highly-doped, electronically conductive form, this porous metal model applies, and oxidation does, indeed, occur throughout the bulk of the polymer (4). The bulk of the evidence indicates, however, that this mechanism is not applicable to the electronically insulating state (5,6,20). Nevertheless, it is clear that at some point a transition between the interfacial and bulk mechanisms must occur. We discuss the potential region of this transition later in this paper.

We have used a series of chronopotentiometric experiments to distinguish between these three possible transport mechanisms. Figure 4 shows results of chronopotentiometric experiments at electrodes coated with polypyrrole films of various thicknesses; the data are plotted as potential vs. $t^{0.5}$ (Equation 6). All films were equilibrated at a potential of -0.35 V prior to application of the current step.

Several important conclusions can be drawn from the data in Figure 4. First, note that there is a rapid rise in potential at short times associated with the combination of the solution and film resistances. The contribution of the film resistance is clearly seen from the increase in this intercept with increasing film thickness. Second, potential increases linearly

with time at longer times; this linear increase in E is associated with the creation of positively-charged monomer sites in the polymer film. It is important to note that the rate of increase in potential with time is the same for all of the electrodes tested in Figure 4. This means that the concentration of oxidized sites, at any time, is the same for all of these films. This observation allows us to immediately discount the porous metal model (4,9).

If the undoped or lightly-doped material were oxidized uniformly through-out the bulk of the film, then at any time during the current step, the concentration of oxidized sites in a thick film would be lower than the concentration of sites in a thin film; this follows because the volume of the thick film is larger, making the moles per unit volume of oxidized sites in the thick film smaller. The lower concentration of oxidized sites in the thick film would cause the potential for this film to raise more slowly with time, relative to a thin film. Because the rate of increase of potential with time is the same for all of the films, we can discard the porous metal model.

While the data discussed above allow us to reject the porous metal model for films equilibrated at potentials negative of -0.30 V, these data do not tell us whether oxidation begins at the Pt/film or film/solution interfaces (12,13). The short-time chronopotentiometric experiment (18), discussed in the Experimental Section, allows us to distinguish between these two possible oxidation models. Recall that in this method we inject a small amount of anodic charge and follow the potential-time transient associated with double layer charging. The question then becomes - where does this double layer charging occur, at the Pt/film interface or at the film/solution interface? If double layer charging occurs at the Pt/film interface then it is reasonable to assume that oxidation begins at this interface. Likewise, if

double layer charging occurs at the film/solution interface, then it is reasonable to assume that oxidation begins at this interface.

The key to determining which interface is charged lies in the resistive component associated with the charging process. If the Pt/film interface is charged, this resistive term is purely ionic because it is associated with ion transport in the solution and polymer phases. In contrast, if the polymer/film interface is charged, then the resistance associated with this charging process will have both an ionic and an electronic component. The ionic component is associated with ion transport in the solution phase; the electronic component is associated with electron transport in the film phase.

As indicated in the Experimental Section, the short-time scale chronopotentiometric can provide the resistive term associated with the double charging process (18). Furthermore, we can by conducting analogous experiments at uncoated electrodes isolate the film component of this resistive term. The question - At which interface does oxidation start? - then boils down to this - Is this film resistive term electronic or ionic in nature? If the film resistive term is ionic, then oxidation begins at the Pt/film interface; if this film resistive term is electronic, then oxidation begins at the film/solution interface.

We have used investigations of the film resistive term as a function of supporting electrolyte concentration to determine whether the film resistive term is ionic or electronic in nature. Note first that we know from independent measurements of the film electronic resistance, that the electronic resistance is independent of supporting electrolyte concentration. Typical data are shown as curve A in Figure 9. In contrast, the resistive term associated with the double layer charging process is, in fact, strongly dependent on

supporting electrolyte concentration (curve B in Figure 9). The data in Figure 9 clearly show that the film resistive term associated with the double layer charging process is ionic in nature. Hence, oxidation must begin at the Pt/polymer interface.

The final question to be addressed is - At what potential does the charge injection mechanism switch to the porous metal-like model? Our chronopotentiometric data provide an answer to this question. Figure 7 shows plots of potential vs. $t^{0.5}$ for current steps at an electrode coated with a 0.26 $\mu$m polypyrrole film which had been equilibrated at various initial potentials. At potentials negative of ca. -0.30 V, the data agree with the simple diffusion model (Equation 6); i.e. a linear increase in potential with $t^{0.5}$ is observed. (We will have more to say about the slopes of these linear portions later in this paper.) Note, however, that at more positive potentials, upward curvature in the potential vs. $t^{0.5}$ plot is observed (Figure 7).

The upward curvature in the potential vs. $t^{0.5}$ plots, indicates that the concentration of oxidized sites increases more rapidly with time than can be accounted for by the simple diffusion model (Equation 6). It seems likely that this nonlinear raise indicates that, at these more positive potentials, oxidized sites are now being produced in the bulk polymer as well as at the Pt/polymer interface. If this interpretation is correct, then it would be reasonable to assume that the film must show a dramatic increase in electronic conductivity in the potential regime where oxidation in bulk is allowed (above ca. -0.30 V, see Figure 7).

To test this hypothesis, we made measurements of film electronic conductivity (using the cell shown in Figure 1) as a function of applied potential. The data obtained are shown in Figure 8. As expected, conductivity does, indeed, increase dramatically at potentials

positive of -0.30 V. Murray et al. have obtained analogous results (22). These data support the assertion that the upward curvature observed in Figure 7 marks the transition from a simple interfacial diffusion model (Equation 6) to the porous metal model (4,9), which allows for oxidation throughout the bulk of the polymer.

Measurement of Apparent Diffusion Coefficients and Exchange Current Densities. The experiments discussed above indicate that, in agreement with our previous investigations, lightly doped polypyrrole behaves like a redox polymer (5,6). Hence it should be possible to ascribe an apparent diffusion coefficient to the diffusive transport of charge from the Pt/polymer interface into the bulk polymer. As is typically the case for redox polymers, the magnitude of this apparent diffusion coefficient can be limited by electron hopping between redox sites in the film, concomitant ionic diffusion, or some combination of these two processes (10,11).

To ascertain whether electron hopping or ionic diffusion is rate limiting, we have conducted current step experiments at a polypyrrole film-coated electrode in solutions containing various concentrations of supporting electrolyte. The film was 0.26 $\mu$m thick and the electrode was equilibrated, in each case, at a potential of -0.35 V. Plots of potential vs. $t^{0.5}$ obtained from these current step experiments are shown in Figure 10.

As might be expected, the intercepts in these potential vs. $t^{0.5}$ plots increase with decreasing electrolyte concentration (Figure 10); this increase in intercept reflects an increase in solution and film ionic resistance at low electrolyte concentrations. However, the slopes of these plots are independent of electrolyte concentration. Since the slope is proportional to the rate of the charge transport process (Equation 6), these data indicate that the rate of

charge transport in the film is independent of supporting electrolyte concentration.

We have shown that the concentration of excess electrolyte in polypyrrole increases with the concentration of supporting electrolyte in the contacting solution phase (6). Hence, if the rate of charge transport were limited by the rate of ion transport, we would expect that the rate would increase with the concentration of supporting electrolyte. That this is clearly not the case (Figure 10), indicates that electron hopping rather than ionic diffusion limits the rate of charge transport in lightly doped polypyrrole.

We have used Equation 6 in conjunction with the potential vs. $t^{0.5}$ data (Figures 4, 8, and 10), and the Nernst plot shown in Figure 5 to calculate apparent diffusion coefficients associated with electron hopping in our lightly-doped polypyrrole films. Table I shows the effect of the amplitude of the current step on the value of the apparent diffusion coefficient. If the simple diffusive model presented above is correct (Equation 6), the apparent diffusion coefficient should be independent of the magnitude of the current step. Table I shows that this is, indeed, the case.

Table II shows the effect of polymer film thickness on the apparent diffusion coefficient. Again, if the model developed here is correct, the apparent diffusion coefficient should be independent of film thickness. Table II shows that this in, indeed, the case. Furthermore, as indicated above, the independence of the slope of the potential vs. $t^{0.5}$ plot on electrolyte concentration (Figure 10) suggests that the apparent diffusion coefficient does not depend on the concentration of electrolyte. Table III shows that this is also true.

Table IV shows the effect of the applied equilibrium potential (i.e. the doping level) on the apparent diffusion coefficient. The apparent diffusion coefficient is independent of

applied potential in the most negative potential regime (-0.5 V to ca. -0.4 V). Mao and Pickup have observed analogous results (23). However, at more positive potentials, the apparent diffusion coefficient increases markedly with potential.

The increase in apparent diffusion coefficient shown in Table IV reflects doping-induced changes in the structure of the polymer. For example, doping introduces ionic sites inti the polymer film. This causes the film to imbibe solvent and expand (24). This increase in void volume is undoubtedly responsible for the increase in apparent diffusion coefficient shown in Table IV.

Finally, it is of interest to compare the apparent diffusion coefficient values obtained here with values obtained in our previous investigations (5,6). The polypyrrole films for these previous investigations were synthesized in acetonitrile solutions which contained no deliberately-added water (5,6). In contrast, the films used here were synthesized in acetonitrile which contained 2 % added water (14-16). The rate of charge transport in films synthesized in acetonitrile containing 2 % water (Tables I-IV) are significantly lower than the rate of charge transport in films synthesized in acetonitrile containing no deliberately-added water (5,6). Indeed, the apparent diffusion coefficients shown in Tables I through IV are about an order of magnitude smaller than films synthesized in the absence of deliberately-added water (5,6).

This difference in apparent diffusion coefficient can be conveniently visualized via the cyclic voltammetric data. Voltammetric currents obtained from films synthesized in the absence of deliberately-added water (e.g. Figure 1 in (6)) are dramatically higher than the

voltammetric currents obtained here (e.g. Figure 6). Furthermore, in reference (6) we were forced to model the E vs. t data using a finite diffusion model, whereas in this study, data from films of the same thickness could be treated using a semi-infinite diffusion model.

We will soon present results of infra red analyses of polypyrrole films synthesized in rigorously-dried acetonitrile and in acetonitrile solutions containing measured quantities of water (25). These investigations have shown that polypyrrole synthesized in the presence of deliberately-added water contains higher concentrations of oxygen-containing defects (e.g. carbonyl and hydroxide) than polypyrrole synthesized in rigorously-dried acetonitrile (25). These defect sites may account for the slower charge-transport in the films investigated here. The bottom line is - if facility of charge-transport is important, we recommend against adding water to the polymerization solutions.

Table III also presents exchange current densities obtained from the intercepts of the potential vs. $t^{0.5}$ plots. To our knowledge, these are the first exchange current densities for the polypyrrole oxidation process to be presented in the literature to date. The magnitude of the exchange current density is reasonably high. For example, the exchange current densities shown in Table III are roughly equivalent to the exchange current density for the $H^+/H_2$ redox couple (in $H_2SO_4$) on Pt (26). However, these exchange current densities are several orders of magnitude lower than densities obtained for simple outer-sphere redox couples. We suggest that the sluggishness observed for the polypyrrole oxidation process is caused by the alterations in bond length associated with the conversion of the polymer from the benzoid (reduced) to quinoid (oxidized) forms (27,28).

## CONCLUSIONS

We have shown that when undoped polypyrrole is oxidized electrochemically, the oxidation process begins at the polymer/electrode interface and propagates to the polymer/solution interface. We have also shown that the rate of this oxidation process is slower for films synthesized in acetonitrile solutions containing deliberately-added water than in films synthesized in rigorously-dried acetonitrile (5,6). Finally, we report the first exchange current densities associated with the electrochemical oxidation of polypyrrole.

ACKNOWLEDGEMENTS - This work was supported by the Office of Naval Research and the Air Force Office of Scientific Research.

## REFERENCES


1. Chiang, C. K.; Druy, M. A.; Gau, S. C.; Heeger, A. J.; Louis, E. J.; MacDiarmid, A. G.; Park, Y. W.; Shirakawa, H. J. Am. Chem. Soc., **1978**, 100, 1013.

2. Diaz, A. F.; Kanazawa, K. K.; Gardini, J. P.; J. Chem. Commun., **1979**, 635.

3. Martin, C. R.; Tierney, M. J.; Cheng, I. F.; Duke, L. V.; Cai, Z.; McBride, J. R.; Brumlik, C. R. Polymer Preprints, **1989**, 30, 424.

4. Cai, Z.; Martin, C. R. J. Electroanal. Chem., **1990**, 35, 424.

5. Penner, R. M.; Martin, C. R. J. Phys. Chem., **1989**, 93, 984.

6. Penner, R. M.; Dyke, L. V.; Martin, C. R. J. Phys. Chem., **1988**, 92, 5274.

7. Genies, E. M.; Pernaut, J. M. Synthetic. Metals, **1985**, 10, 117.

8. Mao, M.; Pickup, P. G.; J. Phys. Chem., **1989**, 93, 6480.

9. Posey, F. A. and Morozumi, T. J. Electrochem. Soc., **1966**, 113, 176.

10. Martin, C. R.; Rubinstein, I.; Bard, A. J. J. Am. Chem. Soc., **1982**, 104, 4817.

11. Kaufman, F. B.; Engler, E. M. J. Am. Chem. Soc., **1979**, 101, 547.

12. Lee, C.; Juhyoun, K.; Bard, A. J. J. Electrochem. Soc., **1989**, 136, 3720.

13. Tezuka, Y.; Aoki, K. J. Electroanal. Chem., **1989**, 273, 161.

14. Diaz, A. F.; Hall, B. IBM J. Res. Dev., **1983**, 27, 342.

15. Kanazawa, K. K.; Diaz, A. F.; Gill, W. D.; Grant, P. M.; Street, G. B.; Gardini, G. P.; Kwak, J. I. Synth. Met., **1980**, 1, 329.

16. Street, G. B.; Lindsey, S. E.; Nazzal, A. J.; Wynne, K. J. Mol. Cryst. Liq. Cryst., **1985**, 118, 137.

17. Street, G. B.; Clarke, T. C.; Geiss, R. H.; Lee, V. Y.; Nazzal, A.; Pfluger, P.; Pletcher, D.; J. Electroanal. Chem. Interfacial Electrochem. **195**, 177, 229.

18. Cai, Z.; Liu, C.; Martin, C. R. J. Electrochem. Soc., **1989**, 136, 3356.

19. Bard, A. J.; Faulkner, L. R. Electrochemical Methods, Wiley, New York, **1980**, p. 255.

20. Bard, A. J.; Faulkner, L. R. Electrochemical Methods, Wiley, New York, **1980**, p. 109.

21. Pickup, P. G.; Osteryoung, R. A. J. Electroanal. Chem, **1985**, 195, 271.

22. Feldman, B. J.; Burgmayer, P.; Murray, R. W. J. Am. Chem. Soc., **1985**, 107, 872.

23. Mao, M.; Pickup, P. G. J. Am. Chem. Soc., **1990**, 112, 1776.

24. Baugman, R. H.; Shacklette, L. W.; Elsenbaumer, R. L.; Plichta, E. J.; Becht, C. Second International Symposium on Molecular Electronics and Biocomputers, Moscow, USSR, September 1989, Kluwer Academic Publishers, in press.

25. Lei, J.; Liang, W.; Martin, C. R., in preparation.

26. Bockris, J. O. M.; Reddy, A. K. N. Modern Electrochemistry, Plenum Press, New York, **1977**, Vol. 2, p. 878.

27. Furukawa, Y.; Tazawa, S.; Fujii, Y.; Harada, I. Synth. Met., **1988**, 24, 329.

28. Bredas, J. L.; Street, G. B., Acc. Chem. Res., **1985**, 18, 309.

Table I. Effect of the amplitude of the applied current step on the apparent diffusion coefficient ($D_e$) in polypyrrole film.

| Step-size ($\mu A/cm^2$) | 160 | 240 | 320 | 480 | 640 |
|---|---|---|---|---|---|
| $D_e x10^{10}$ ($cm^2/s$)[a] | 1.2±0.2 | 1.2±0.1 | 1.2±0.1 | 1.1±0.1 | 1.2±0.1 |

[a] Each datum is the average of four measurements

Table II. Influence of film thickness on the apparent diffusion coefficient ($D_e$) in polypyrrole film.

| Film thickness ($\mu$m) | 0.13 | 0.26 | 0.39 | 0.52 | 0.78 |
|---|---|---|---|---|---|
| $D_e \times 10^{10}$ ($cm^2/s$)[a] | 1.1±0.2 | 1.2±0.1 | 1.2±0.1 | 1.2±0.1 | 1.3±0.1 |

[a] Each datum represents the average of four measurements (two films, two measurements for each film).

Table III. Dependence of the apparent diffusion coefficient ($D_e$) and exchange current density ($i_o$) on the concentration of external electrolyte.

| Electrolyte Conc. (M) | 0.025 | 0.050 | 0.10 | 0.20 |
|---|---|---|---|---|
| $D_e \times 10^{10}$ ($cm^2/s$) | 1.4±0.2 | 1.4±0.2 | 1.4±0.2 | 1.3±0.2 |
| $i_o$ ($mA/cm^2$) | 5±3 | 4±2 | 5±2 | 3±1 |

[a] Each Datum is the average of three measurements.

Table IV. Effect of the initial electrode potential on the doping level and apparent diffusion coefficient in polypyrrole.

| E(0) (V) | -0.50 | -0.45 | -0.425 | -0.40 | -0.35 | -0.30 |
|---|---|---|---|---|---|---|
| Doping level (%) | 0.021 | 0.055 | 0.089 | 0.14 | 0.32 | 0.90 |
| $D_e \times 10^{10}$ ($cm^2/s$)[a] | 0.65±0.1 | 0.71 | 0.75 | 0.85 | 1.5 | 2.5 |

[a] Each datum is an average of four measurements.

## FIGURE CAPTIONS

Figure 1. Bipotentiostatic circuit used for in situ measurement of film electronic conductivity.

Figure 2. Potential-time transients associated with small amplitude (10 $\mu$A, 90 $\mu$sec) current pulses applied to a 0.78 $\mu$m-thick polypyrrole film-coated Pt electrode. Initial potential was -0.35 V. Supporting electrolyte was a) 0.1 M and b) O.2 M $Et_4NBF_4$ in $CH_3CN$.

Figure 3. Potential-time transients associated with currents steps of 0.32 mA $cm^{-2}$ at Pt electrodes coated with various thicknesses of polypyrrole films. Initial potential in each case was -0.35 V. Supporting electrolyte concentration was 0.2 M. Film thicknesses as shown.

Figure 4. Plots of E vs $t^{0.5}$ for data shown in Figure 3.

Figure 5. Plot of applied equilibrium potential vs. log of the concentration of oxidized monomer sites in a 0.26 $\mu$m polypyrrole film. Electrolyte as per Figure 3.

Figure 6. Cyclic voltammogram for a 0.52 $\mu$m-thick polypyrrole film. Electrolyte as per Figure 3. Scan rate = 10 mV $sec^{-1}$.

Figure 7. Plots of potential vs. $t^{0.5}$ for chronopotentiometric experiments conducted at various initial potentials. Film thickness = 0.26 $\mu$m. Electrolyte and current step as per Figure 3.

Figure 8. Variation of electronic conductivity for polypyrrole on equilibrium electrode potential. Electrolyte as per Figure 3.

Figure 9. Effect of supporting electrolyte concentration on the film conductivity. A. Conductivity measured using the small amplitude current pulse technique. B. Electronic conductivity measured using the apparatus shown in Figure 1. Initial potential = -0.35 V.

Figure 10. Plots of potential vs. $t^{0.5}$ from chronopotentiometric experiments on a 0.26 $\mu$m polypyrrole film in contact with solutions of various supporting electrolyte concentration. Initial potential = -0.35 V. Current step = 0.30 mA $cm^{-2}$.

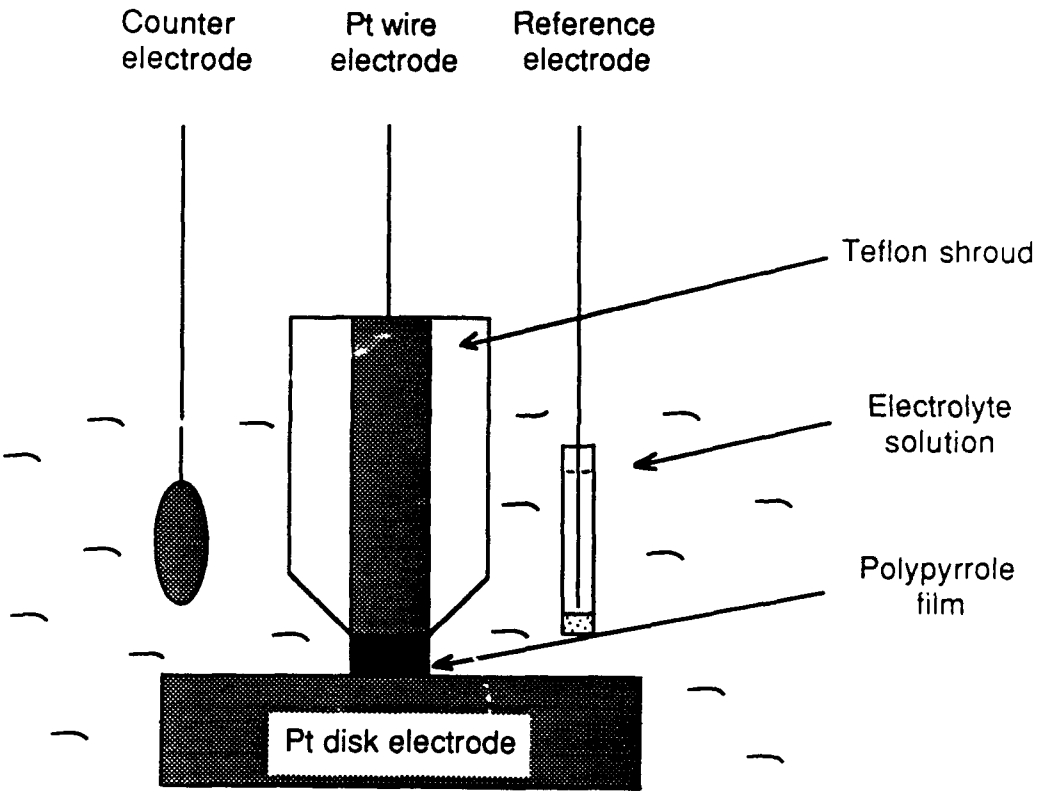
Counter electrode
Pt wire electrode
Reference electrode
Teflon shroud
Electrolyte solution
Polypyrrole film
Pt disk electrode

Fig 1

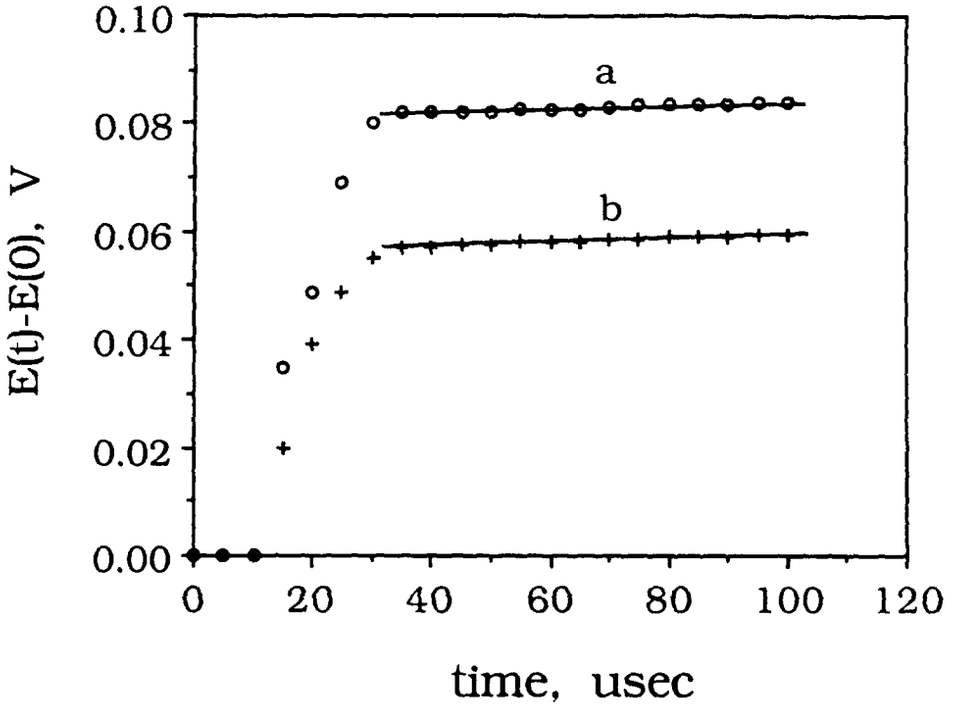


Fig 2.

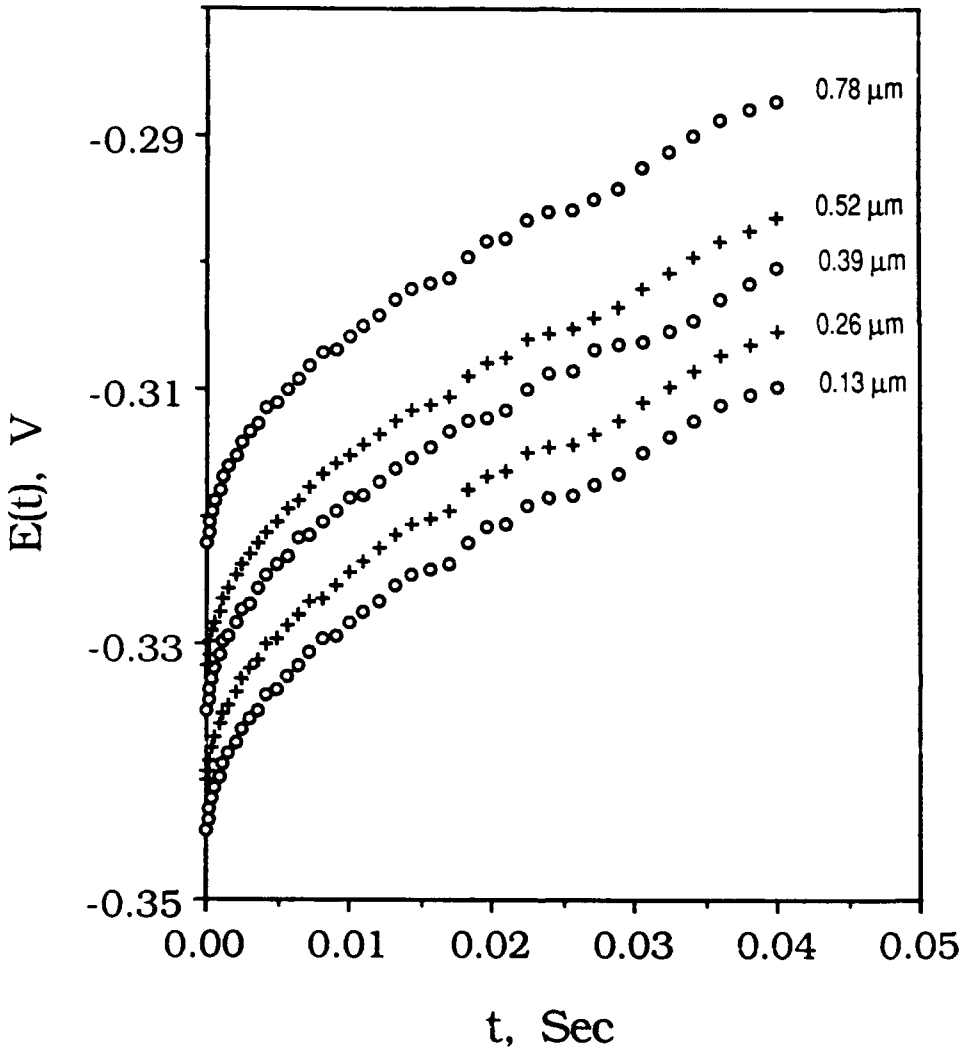
0.78 µm
0.52 µm
0.39 µm
0.26 µm
0.13 µm
-0.29
-0.31
-0.33
-0.35
E(t), V
0.00
0.01
0.02
0.03
0.04
0.05
t, Sec

Fig3

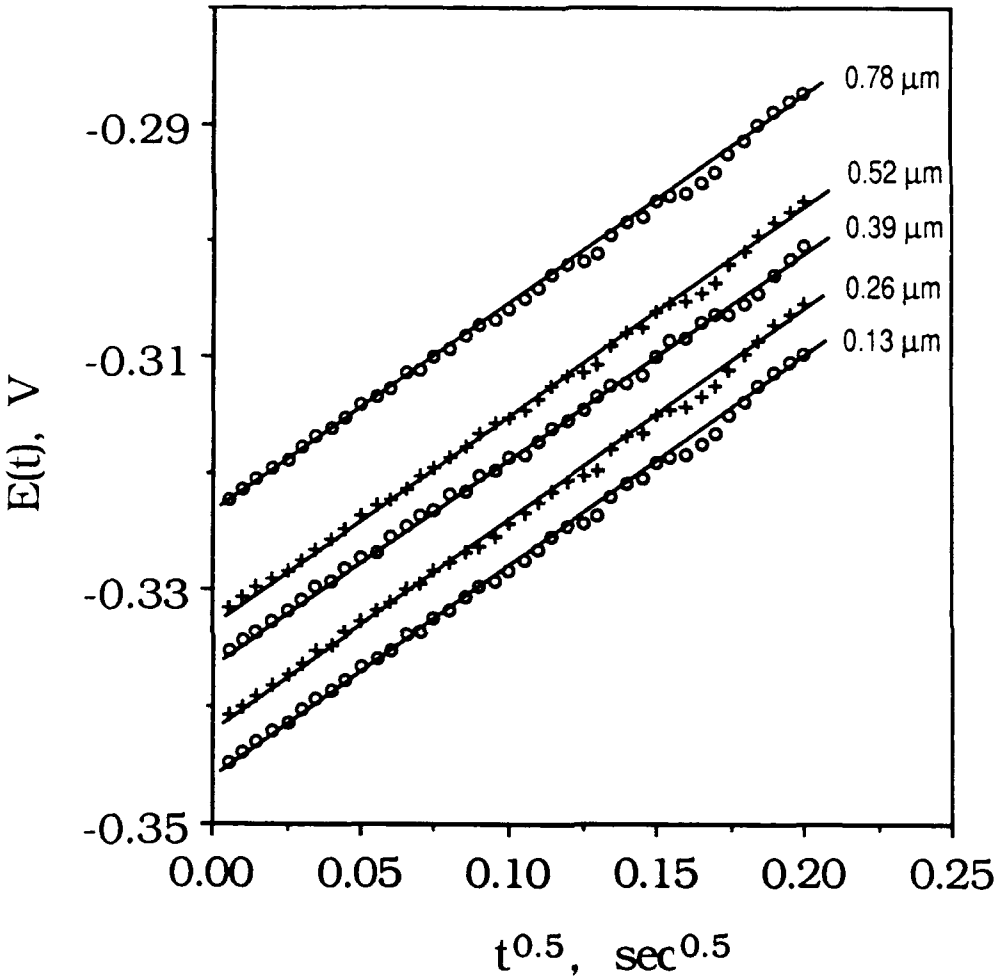
0.78 µm
0.52 µm
0.39 µm
0.26 µm
0.13 µm
-0.29
-0.31
-0.33
-0.35
E(t), V
0.00
0.05
0.10
0.15
0.20
0.25
t^0.5, sec^0.5

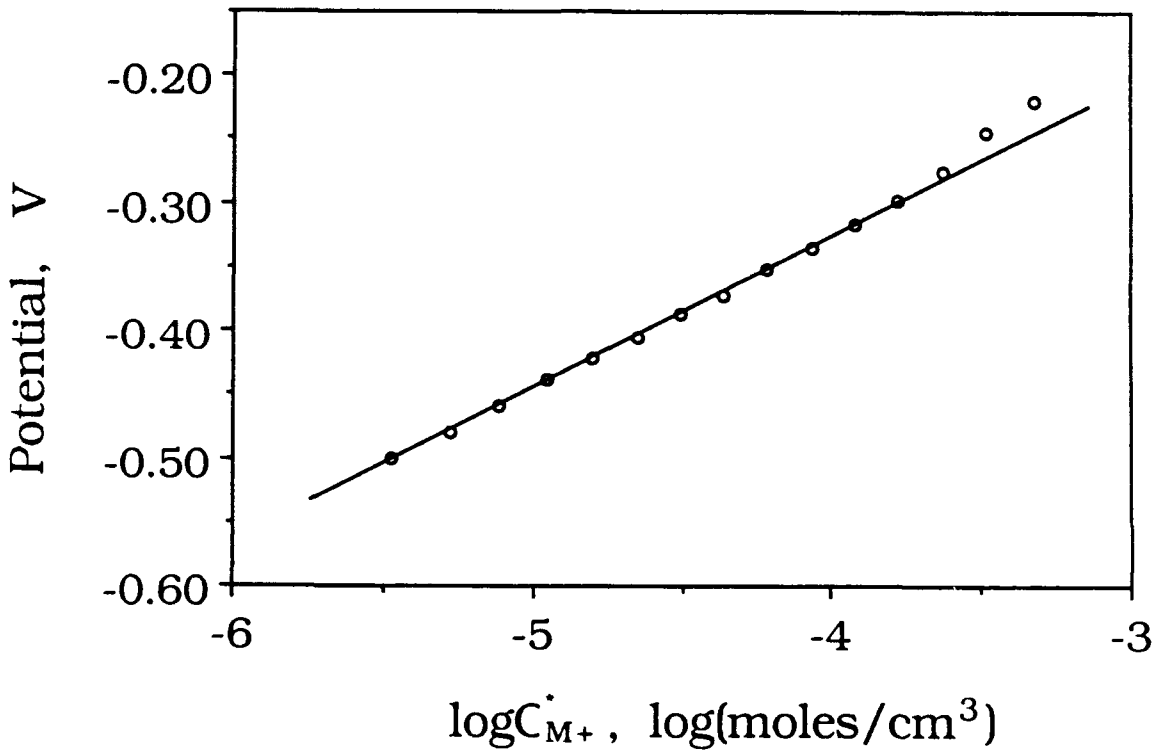
-0.20
-0.30
-0.40
-0.50
-0.60
Potential, V
-6
-5
-4
-3
logC*M+ , log(moles/cm3)

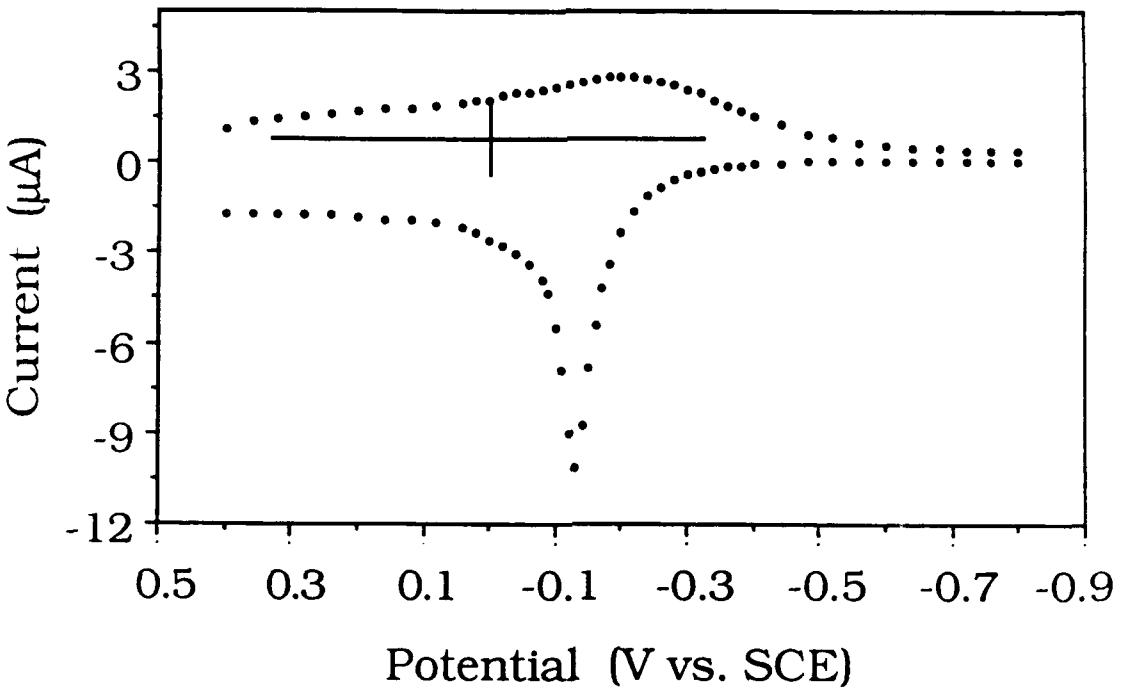
3
0
-3
-6
-9
-12
Current (μA)
0.5
0.3
0.1
-0.1
-0.3
-0.5
-0.7
-0.9
Potential (V vs. SCE)

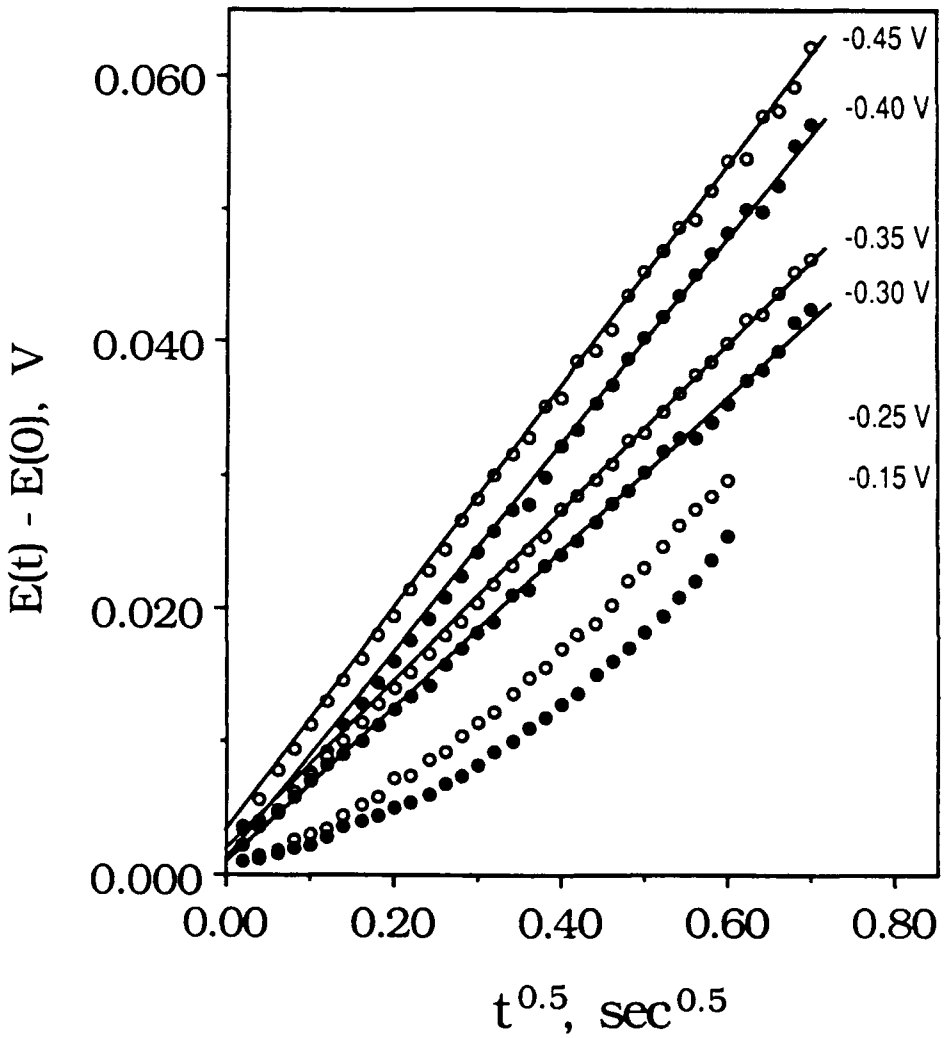
0.060
0.040
0.020
0.000
0.00
0.20
0.40
0.60
0.80
E(t) - E(O), V
t^0.5, sec^0.5
-0.45 V
-0.40 V
-0.35 V
-0.30 V
-0.25 V
-0.15 V

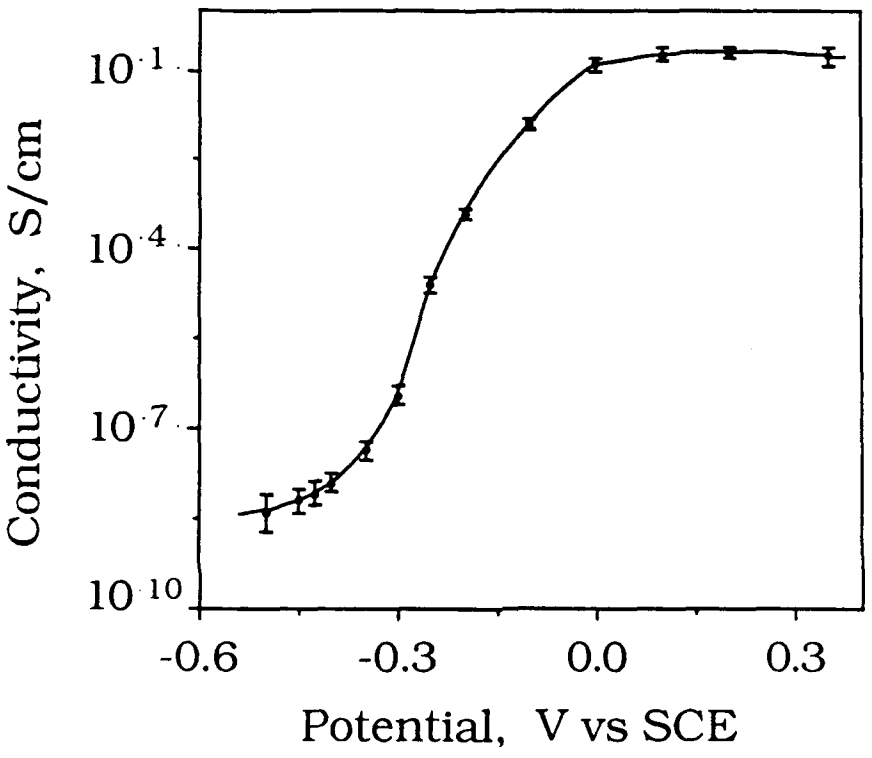
Conductivity, S/cm
10 -1
10 -4
10 -7
10 -10
-0.6
-0.3
0.0
0.3
Potential, V vs SCE

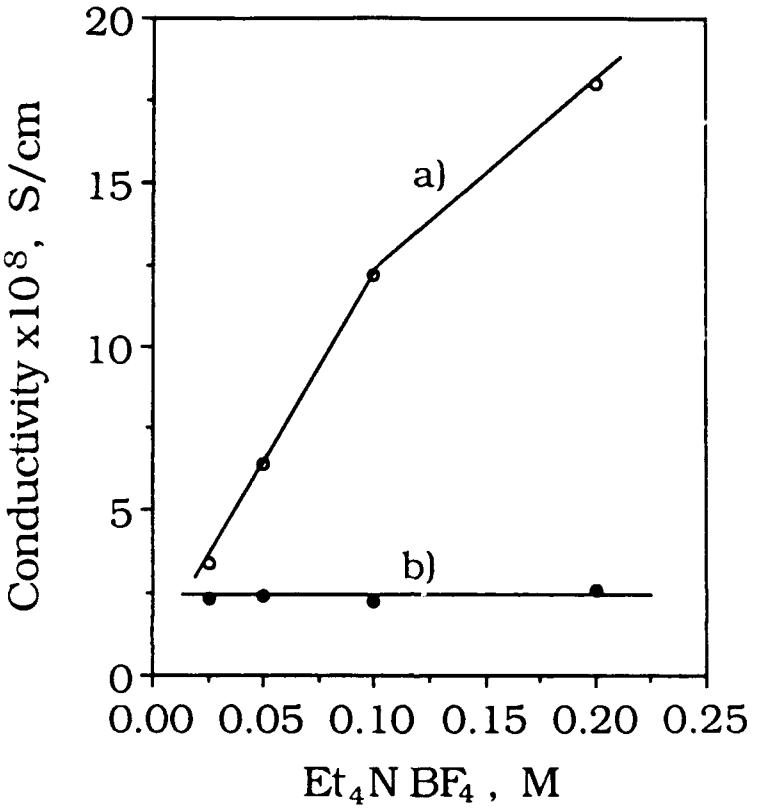
20
15
10
5
0
Conductivity x10$^8$, S/cm
a)
b)
0.00 0.05 0.10 0.15 0.20 0.25
$Et_4N\,BF_4$ , M

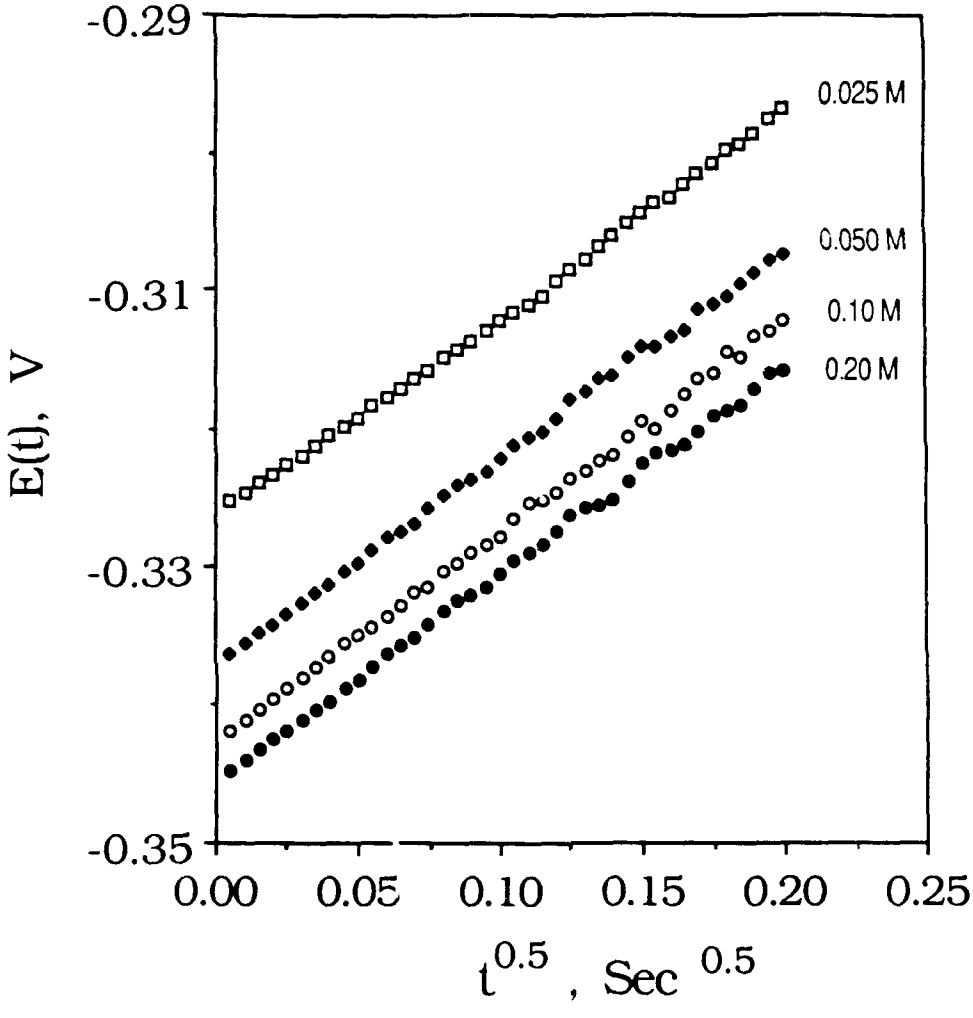
-0.29
-0.31
-0.33
-0.35
E(t), V
0.00
0.05
0.10
0.15
0.20
0.25
t^0.5 , Sec^0.5
0.025 M
0.050 M
0.10 M
0.20 M